2017 International Nuclear Atlantic Conference - INAC 2017
Belo Horizonte, MG, Brazil, October 22-27, 2017
ASSOCIAÇÃO BRASILEIRA DE ENERGIA NUCLEAR - ABEN

Agência Brasileira do ISBN
ISBN 978-85-99141-07-6
9 788599 141076

CHARACTERIZATION OF CRYSTALLINE PHASES OF (U,Er)O2 PELLETS BY X-RAY DIFFRACTION

Alberto E. S. Sansone[1,a], Humberto G. Riella[1,b], and Elita F. U. de Carvalho[1,c]
[1]Instituto de Pesquisas Energéticas e Nucleares (IPEN/CNEN)
Av. Professor Lineu Prestes 2242
05508-000 São Paulo, SP
[a]alberto.sansone@usp.br, [b]riella@enq.ufsc.br, [c]elitaucf@ipen.br

ABSTRACT

Optimization of nuclear fuel for use in pressurized water reactors can be achieved by obtaining higher burnups. This, however, requires the excess reactivity caused by increasing the fuel's enrichment to be taken into account, which can be done by introducing burnable absorbers into the UO_2 fuel pellets themselves. Some of the rare earth elements have thermal and mechanical properties that make them appropriate for use inside the reactor. In order to characterize the microstructure of erbium-doped UO_2 fuel, sintered UO_2-Er_2O_3 pellets were prepared, with Er_2O_3 content ranging from 1.0 to 9.8wt%, and analyzed by X-ray diffraction to determine whether the composite formed solid solutions and, if so, evaluate the lattice parameter as a function of erbia concentration. While XRD analysis showed the Er_2O_3 completely dissolved in the UO_2 powder, it also evidenced the emergence of a second fluorite-type phase, whose phase fraction increases and lattice parameter decreases with increasing erbia concentration. Analysis of the diffraction patterns showed this emerging phase has the same crystalline structure as the host lattice, but with a smaller lattice parameter, and a smaller domain size. These results are compatible with the phenomenon of defect segregation, which consists in the formation of microdomains with a higher concentration of defects.

1. INTRODUCTION

With the ever-growing need of reliable clean energy, developing new sources and improving the efficiency of old ones is of utmost importance in today's world, and nuclear energy can fill this role since it can be both efficient and light on greenhouse gas emission, compared to other established sources [1]. But while the generation of nuclear energy is clean by itself, there are safety and waste disposal issues that need to be addressed. Because of that, optimizing both the efficiency and safety of nuclear fuels' cycles is a constant effort on the nuclear science research front. One of the main research lines on nuclear fuels concerns itself with extending fuels' burn-cycle length through higher burnups [2]. It is well known that waste processing is a significant factor in the total operation cost of nuclear reactors. Therefore, prolonging the burn-cycle period and thus reducing the core reloading frequency can significantly optimize the nuclear fuel's cycle, and has been one of the main goals of current nuclear fuel R&D. One of the approaches that allow to safely increase the fuel's enrichment is the use of the so-called burnable absorbers directly into the fuel pellets. A burnable absorber is an element whose neutron absorption cross-section is high compared to that of the nuclear fuel, but such that the products of the absorption reaction have low neutron-absorption cross-section themselves [3]. This way, the amount of absorption-prone material in the core reduces as the fuel burns. For large-scale commercial application, it is also desirable that the elements used

as neutron absorbers have large enough natural occurrence and thermal and mechanical properties adequate for use inside the core. Among the rare-earth elements, gadolinium (Gd) and erbium (Er) fill the requirements to be used as burnable absorbers in pressurized water reactors, with gadolinium being already widely used. Other elements can be used as burnable absorbers as well, and erbium, because of its similarities with gadolinium, it is seen as a possible alternative. One of its advantages is that it is more adequate for longer burn-cycles than gadolinium [4].

Due to the influence that physical and chemical characteristics of erbium-doped fuel may have over its performance in-reactor, it's desirable to better understand its physical and chemical properties, including its microstructure, and how they may be affected by different preparation routes.

2. OBJECTIVES

This work aims to study, by x-ray diffraction, the nanostructural characteristics of crystalline phases formed by sintered pellets of mixture UO_2-Er_2O_3, with Er_2O_3 content varying from 1.0 to 9.8 wt%.

3. METHODS

In order to characterize the effect of erbia doping in uranium dioxide's microstructure, urania-erbia (UO_2-Er_2O_3) mixtures were prepared, with erbia ranging from 0.0 to 9.8wt% in concentration. The powders were then pressed and sintered. After that, the pellets were ground and the powder obtained was analyzed by x-ray diffraction.

3.1. Pellets

The UO_2 powder used was given by Indústrias Nucleares do Brasil (INB); the Er_2O_3 powder was obtained from Alfa Aesar.

The powder mixture for each pellet had a total mass of 5.20g, and consisted of 0.2 wt% of aluminum stearate, x wt% of Er_2O_3 ($x = 0.0$, 1.0, 2.5, 4.0 and 9.8), with the remaining composition being INB's UO_2 powder; all these powders were mixed in a Turbula for 1h. The mixtures were pressed and then sintered at 1700°C in a H_2/Ar reducing atmosphere for 3h.

3.2. X-ray diffraction

The diffraction patterns from the powder samples were obtained at room temperature using a Bruker's D8 Advance diffractometer, with both anti-scattering and divergent slits of 1.0mm and a 0.4mm receiving slit, using a monochromatic Cu-Kα radiation. The measuring step was 0.02°, with counting time of 10s at each step.

For the analysis of the diffraction data, the software GSAS-II [6] was used.

4. RESULTS

Both urania and erbia powders used to make the pellets had their purity assessed through XRD. Erbia's diffractogram reflections matches a structure with space group Ia-3, with code 1534952 from ICSD [5], while uranias's diffraction pattern contains UO_2 (ICSD code 246851) and small fractions of U_4O_9 (ICSD code 246852), U_3O_7 (ICSD code 246853) and U_3O_8 (ICSD code 246854). Quantitative phase analysis showed the content of non-cubic phases (U_3O_7 and U_3O_8) to be less than 5%.

The diffraction patterns obtained for all the samples are shown in Fig. 1, together with the reflection positions of the UO_2 and Er_2O_3 powders used. (All the plots in this work were made using the package Matplotlib [7] for Python 2.7 [8].) No Er_2O_3 peaks were observed in the doped pellets' diffraction patterns, which means the erbia powder dissolved in the urania powder.

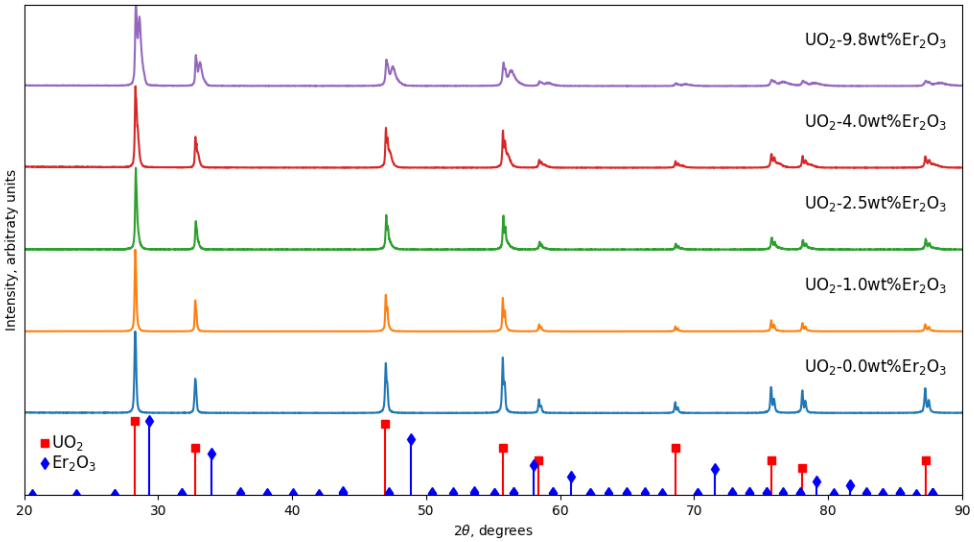

Figure 1: Diffraction patterns of the pellets analyzed. At the bottom, the reflections for the structures of the UO_2 and Er_2O_3 powders used to make the pellets.

However, instead of forming a single phase solid solution, two phases can be observed. The second phase has the same set of reflection as the first one, but shifted to the right, i.e. the second phase also has a fluorite-type structure, but with a smaller lattice parameter. The presence of a second phase is more evident for pellets with higher amounts of erbia, since the intensities of the emerging phase's reflections increase along with the erbia content in the pellet, which means the second phase's fraction increases as a function of erbia content. The peaks of this second phase can be resolved visually for the pellets with doping of 4.0 and 9.8 wt%Er_2O_3. For the 1.0 and 2.5 wt%Er_2O_3 pellets, even thought the second phase's maxima do not appear separated from the maxima of the first phase, they still

can be seen as "tails" to the right of each peak. For the pellet with 1.0 wt%Er_2O_3, these tails are less evident, but their effects on the peak profiles can be perceived, specially at higher angles, when comparing the diffraction patterns for the doped and undoped pellets, as evidenced in Fig. 2(a). Therefore, when determining the lattice parameters for the erbium-doped pellets, the existence of two phases (α and β) was assumed even for 1.0 and 2.5 wt%Er_2O_3 concentrations, although these two pellets could be considered as a single phase with low homogeneity degree [9]. For the pellets with 4.0 and 9.8 wt%Er_2O_3, the peaks of the emerging phase can be seen separated from the first phase, as Fig. 2(b) shows.

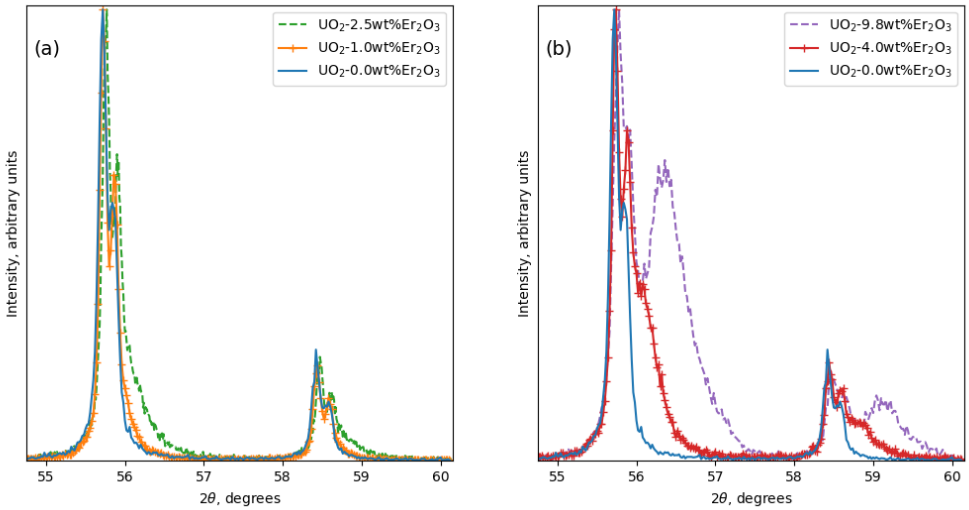

Figure 2: Comparisons of the diffraction patterns from the undoped UO_2 pellet with the patterns from the pellets with doping of (a) 1.0 and 2.5 wt%Er_2O_3 and (b) 4.0 and 9.8 wt%Er_2O_3. Peaks of a emerging second phase can be seen to the right of the undoped pellet's diffraction peaks, and their intensities increase along with the concentration of erbia in the pellet.

For the Rietveld refinement, the structures used were derived from the structure with code 1541596 from the Crystallography Open Database [10].

The results of the Rietveld refinements, all of them compiled on Table 1, including the lattice parameters and phase fractions obtained, as well as the refinements' residuals [13], show that α's lattice parameter does not deviate more than 1% from the lattice parameter of the undoped UO_2 pellet; on the other hand, β's lattice parameter decreases with increasing erbia concentration. Furthermore, the weight fraction results indicate β phase becomes more abundant as the erbia content increases. It can be seen on R_{F^2} values that, while α-phase seem to fit the fluorite reflections' positions and intensities, some of β's R_{F^2} are larger than 5%, indicating that this phase may be a fluorite deformation, such as a rhombohedral or tetragonal [11, 12]. As for β-phase's R_{F^2} value for the 9.8 wt%Er_2O_3 pellet, it can be seen in the diffraction pattern that β's reflections intensities have long

tails compared to α's, so that part of β's reflections may not be included in the refinement software's evaluation of R_{F^2}, which might explain why β's R_{F^2} drops to less than 5% again [13].

Table 1: Summary of the Rietveld refinements results. R_{wp} is the intensity-weighted residual factor obtained directed from the quantity minimized by the Rietveld refinement; the goodness of fit, GOF, measures how much the R_{wp} approaches the best possible fit, for which would be GOF = 1.0; and R_{F^2} is the reflection based residual that indicates if the crystallographic models fit the observed reflections [13].

wt%Er_2O_3	Phase	Lattice parameter (Å)	Weight fraction	R_{F^2}(%)	R_{wp}(%)	GOF
0.0	-	5.47084	—	4.688	15.433	1.23
1.0	α	5.47021	0.654	2.990	10.684	1.26
	β	5.46170	0.346	3.334		
2.5	α	5.47048	0.611	3.815	15.838	1.16
	β	5.44763	0.389	9.764		
4.0	α	5.47004	0.504	3.926	14.570	1.37
	β	5.44265	0.496	11.690		
9.8	α	5.47165	0.252	4.542	12.869	1.47
	β	5.42386	0.748	3.411		

There are reports of single phase solid-solution formation for UO_2-Er_2O_3 system [14, 15], but with distinct preparation procedures, e.g. heat treatment or mixing technique. The different heat treatment and the dry processing alone could explain why a single phase solid-solution was not achieved. The phase separation in the system UO_2-Er_2O_3 observed here was already seen for analogous mixtures of urania and other compounds, including rare-earth oxides [17]. For the mixture UO_2-Nd_2O_3, Desgranges *et al.* [22, 23] reported an effect similar to what was observed in this work and proposed the existence of a miscibility gap for the concentration range of $6 - 20$ wt%Nd_2O_3 where two cubic phases can also be seen with XRD. This phenomenon is usually explained [24] by considering two mechanisms: the formation of oxygen vacancies and the oxidation of uranium ions from U^{4+} to U^{5+} (or U^{6+}, more rarely) – both mechanisms consequences of the incorporation of erbium ions (of valence 3^+) in sites of uranium ions (of valence 4^+); and both have as a driving force the maintenance of electroneutrality in the host lattice [17].

Because of the small ionic radius of U^{5+} (or U^{6+}) compared to U^{4+}, as can be seen in Table 2, the transition $U^{4+} \rightarrow U^{5+}$ causes a deformation in the neighborhood of the uranium site which makes the whole lattice contract in order to reduce the energy introduced by

the defect [18]. The bigger the amount of U^{5+}, i.e. the bigger the number of Er^{3+} ions incorporated into UO_2 lattice, the bigger the contraction in the lattice [19].

Table 2: Radii of ionic species discussed [25].

Ion	Radius(Å)
$^{VIII}U^{4+}$	1.001
$^{VII}U^{5+}$	0.960
$^{VII}U^{6+}$	0.880
$^{VIII}Er^{3+}$	1.004

However, there is a limit to the number of defects a lattice supports. This follows from the site exclusion principle, which states that when a defect occupies a given site in a lattice, a specific number of sites becomes unavailable to defects of the same type of the defect introduced. So when a defect occupies a specific site, the number of available sites for that type of defect is decreased; and as the number of defects approach a saturation limit, new defects are allocated to preferential regions in the lattice, forming a microdomain with a higher concentration of that defect and a different structure [20].

Applying this to the case studied here, the (U,Er)O_2 lattice, as the number of U^{5+} increases (as a result from the incorporation of Er^{3+} ions), microdomains with a higher concentration of U^{5+} are formed. Those would correspond to the β phase observed in the diffraction patterns of the pellets. Indeed, the peak profiles of phase β are broader than α's, indicating the diffraction domains of β are small compared to the diffraction domains of α, which is what would be expected if β represents microdomains segregated from the host lattice α. Also, β's lattice parameter decreases as erbia concentration increases, as shown in Fig. 3(a), indicating β has a higher fraction of oxidized uranium ions (U^{5+} and U^{6+}) compared to α. Finally, the intensities of phase β increase as a function of Er_2O_3 concentration, i.e. the phase fraction of β increases, as can be seen in Fig. 3(b). This is also expected if β indeed consists of segregated microdomains, since a bigger amount of solute (erbium) to be incorporated in the lattice would imply in the formation of a bigger amount of those domains.

So while the small difference between Er^{3+} and U^{4+} ionic radii facilitates the incorporation of Er in UO_2's lattice, the (negative) ionic radius variation caused by the substitution $U^{4+} \rightarrow U^{5+/6+}$ is not well-compensated by the the (positive) difference between $U^{4+} \rightarrow Er^{3+}$, as can be derived from Table 2. This difference can affect the lattice stability [21] and may explain the fluorite phase separation into two new phases observed in the diffraction patterns: the valence transition of uranium ions causes a contraction in the lattice, while the formation of oxygen vacancies results in an expansion. Thus, the competition between oxygen vacancies formation and valence transition $U^{4+} \rightarrow U^{5+}$ forms two domains – a O_v-rich and a U^{5+}-rich one.

Therefore, the results obtained in this work for the urania-erbia system are compatible with the phenomenon of microdomain segregation of defects observed for other materials.

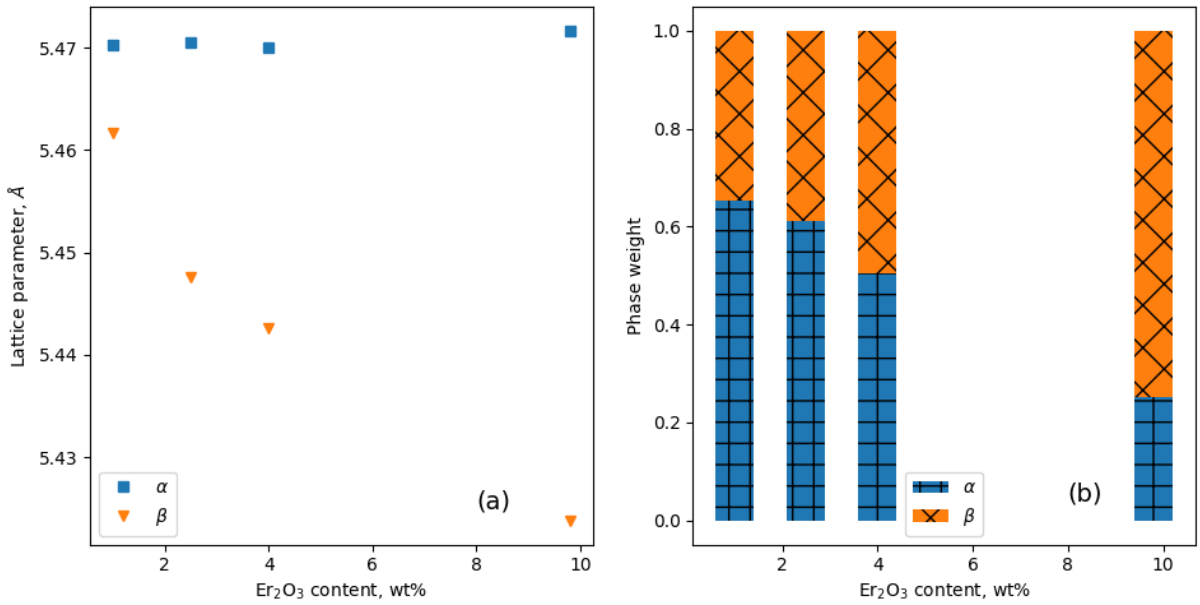

Figure 3: (a) Lattice parameters of phases α and β as a function of erbia content in the pellet. (b) Relative phase fractions in the pellet for each pellet as a function of erbia concentration.

Other methods of characterization should be used to verify these hypothesis. Future studies will analyze the samples through electron microscopy, helping determine if the pellets' microstructure in fact contains domains of deformed fluorite-type structure, giving a more conclusive answer.

5. CONCLUSIONS

The urania-erbia system was studied with Er_2O_3 content ranging from 0.0 to 9.8 wt% in UO_2 pellets sintered in reducing atmospheres at 1700°C for 3h. Inspection of X-ray diffraction patterns from the doped pellets showed no trace of the Er_2O_3 phase, which means the erbium solute atoms were completely incorporated in the UO_2 host lattice. However, the diffraction patterns also evidenced the emergence of a second fluorite-like phase. Rietveld analysis of the patterns showed that the abundance of the emerging phase increases as a function of erbia concentration, while its lattice parameter decreases.

The emergence of this second phase can be attributed to the formation of segregated microdomains with a higher fraction of U^{5+} ions, which form as a way to maintain the electroneutrality of the UO_2 lattice when a erbium ion is incorporated in it by the substitution $Er^{3+} \rightarrow U^{4+}$. The results obtained from the XRD analysis are compatible with this hypothesis, specifically the smaller lattice parameter and domain size of the emerging phase, as well as the fact that its abundance is tied to the amount of solute used in the pellet. Future studies with electron microscopy may help determine conclusively if these mechanisms are indeed taking place in the samples used in this work and causing the

effects observed in the XRD patterns.

ACKNOWLEDGMENTS

This work was financially supported by CAPES-Eletronuclear. The UO_2 powder used was supplied by Indústrias Nucleares do Brasil.

REFERENCES

1. M. Lenzen, "Life cycle energy and greenhouse gas emissions of nuclear energy: A review", *Energy conversion and management*, **49**, pp. 2178–2199, (2008).
2. J. R. Secker, B. J. Johansen, D. L. Stucker, O. Ozer, K. Ivanov, S. Yilmaz and E. H. Young, "Optimum discharge burnup and cycle length for PWRs", *Nuclear Technology*, **151**, pp. 109–119, (2005).
3. R. J. Cacciapouti, R. J. Weader and J. P. Malone, "PWR burnable absorber evaluation", *Nuclear Energy*, **34**, pp. 303–305, (1995).
4. M. Asou and J. Porta, "Prospects for poisoning reactor cores of the future", *Nuclear engineering and design*, **168**, pp. 261–270, (1997).
5. M. Hellenbrandt, "The inorganic crystal structure database (ICSD)present and future", *Crystallography Reviews*, **10**, pp. 17–22, (2004).
6. B. H. Toby and R. B. von Dreele, "GSAS-II: the genesis of a modern open-source all purpose crystallography software package", *Journal of Applied Crystallography*, **46**, pp. 544–549, (2013).
7. J. D. Hunter, "Matplotlib: A 2D graphics environment", *Computing In Science & Engineering*, **9**, pp. 90–95, (2007).
8. G. van Rossum and F. L. Drake Jr, "Python reference manual", (1995).
9. A. A. Rempel and A. I. Gusev, "Preparation of disordered and ordered highly nonstoichiometric carbides and evaluation of their homogeneity", *Physics of the Solid State*, **42**, pp. 1280–1286, (2000).
10. S. Gražulis, A. Daškevič, A. Merkys, D. Chateigner, L. Lutterotti, M. Quiros, N. R. Serebryanaya, P. Moeck, R. T. Downs and A. Le Bail, "Crystallography Open Database (COD): an open-access collection of crystal structures and platform for world-wide collaboration", *Nucleic acids research*, **40**, pp. D420–D427, (2011).
11. P. Herrero, P. Garcia-Chain and R. M. Rojas, "Microstructural characterization of the fluorite phase in the U-La-O system. I. Rhombohedral microdomain formation in (U1-yLay) O2±x 0.56≤ y≤ 0.67", *Journal of Solid State Chemistry*, **87**, pp. 331–343, (1990).
12. C. Rockenhäuser, *Electron Microscopical Investigation of Interdiffusion and Phase Formation at Gd2O3/CeO2-and Sm2O3/CeO2-Interfaces*, Springer (2015).
13. B. H. Toby, "R factors in Rietveld analysis: How good is good enough?", *Powder diffraction*, **21**, pp. 67–70, (2006).
14. S. Yamanaka, K. Kurosaki, M. Katayama, J. Adachi, M. Uno, T. Kuroishi and M. Yamasaki, "Thermal and mechanical properties of (U,Er)O2", *Journal of Nuclear Materials*, **389**, pp. 115–118, (2009).

15. H. S. Kim, Y. K. Yoon and Y. W. Lee, "Defect structures of U1- yEryO2±x solid solutions", *Journal of nuclear materials*, **226**, pp. 206–215, (1995).
16. H. G. Riella, M. Durazzo, M. Hirata and R. A. Nogueira, "UO2-Gd2O3 solid solution formation from wet and dry processes", *Journal of nuclear materials*, **178**, pp. 204–211, (1991).
17. T. Ohmichi, S. Fukushima, A. Maeda and H. Watanabe, "On the relation between lattice parameter and O/M ratio for uranium dioxide-trivalent rare earth oxide solid solution", *Journal of Nuclear Materials*, **102**, pp. 40–46, (1981).
18. L. Minervini and O. Z. Matthew and W. G. Robin, "Defect cluster formation in M 2 O 3-doped CeO 2", *Solid State Ionics*, **116**, pp. 339–349, (1999).
19. A.V. Fedotov and E. N. Mikheev and A. V Lysikov and V. V. Novikov, "Theoretical and experimental density of (U, Gd) O2 and (U, Er) O2", *Atomic Energy*, **113**, pp. 429–434, (2013).
20. R. Catlow, *Defects and Disorder in Crystalline and Amorphous Solids*, Springer Science (2012).
21. J. W. McMurray, D. Shin and T. M. Besmann, "Thermodynamic assessment of the U–La–O system", *Journal of Nuclear Materials*, **456**, pp. 142–150, (2015).
22. L. Desgranges, M. Marcet, Y. Pontillon, F. Porcher, J. Lamontagne, P. Matheron, X. Iltis and G. Baldinozzi, "Evidence of a Biphasic Domain in the UO2-Nd2O3 Diagram at Room Temperature: a Proof for a Miscibility Gap in UO2-Nd2O3 Phase Diagram?", *Solid State Phenomena*, **172**, pp. 624–629, (2011).
23. L. Desgranges, Y. Pontillon, P. Matheron M. Marcet, P. Simon, G. Guimbretiere and F. Porcher, "Miscibility gap in the U–Nd–O phase diagram: a new approach of nuclear oxides in the environment?", *Inorganic chemistry*, **51**, pp. 9147–9149, (2012).
24. M. Razdan and D. W. Shoesmith, "Influence of trivalent-dopants on the structural and electrochemical properties of uranium dioxide (UO2)", *Journal of The Electrochemical Society*, **161**, pp. H105–H113, (2014).
25. R. D. Shannon, "Revised effective ionic radii and systematic studies of interatomic distances in halides and chalcogenides", *Acta crystallographica section A: crystal physics diffraction theoretical and general crystallography*, **32**, pp. 751–767, (1976).